Journal of Applied Polymer Science

Polymorphic Crystallization of Poly(butylene adipate) and Its Copolymer: Effect of Poly(vinyl alcohol)

Zhichao Liang,[1,2,3] Jinjun Yang,[4] Lei Hua,[1] Pengju Pan,[5] Jian Huang,[2] Jianjun Zhang,[2] Hideki Abe,[3] Yoshio Inoue[1]

[1]Department of Biomolecular Engineering, Tokyo Institute of Technology, 4259-B-55 Nagatsuta, Midori-Ku, Yokohama 226-8501, Japan

[2]R&D Center, Yonggao Company, Limited, Daixi Road, Huangyan, Taizhou 318020, China

[3]Bioplastic Research Team, RIKEN Biomass Engineering Program, 2-1 Hirosawa, Wako, Saitama 351-0198, Japan

[4]School of Environmental Science and Safety Engineering, Tianjin University of Technology, Tianjin 300384, China

[5]State Key Laboratory of Chemical Engineering, Department of Chemical and Biological Engineering, Zhejiang University, 38 Zheda Road, Hangzhou 310027, China

Correspondence to: Z. Liang (E-mail: zhichao.liang@yonggao.com) or P. Pan (E-mail: panpengju@zju.edu.cn)

ABSTRACT: The crystallization kinetics and crystalline structure of the biodegradable polymorphic polymers, poly(butylene adipate) (PBA) and poly(butylene adipate-*co*-hexamethylene adipate), in the microparticles and nanoparticles covered by poly(vinyl alcohol) (PVA), and those on the PVA substrate were investigated by differential scanning calorimetry, wide-angle X-ray diffraction, and Fourier transform infrared spectroscopy. Both the polymers crystallized in the particle state and on the PVA substrate showed higher crystallization temperatures in the nonisothermal melt crystallization and shorter crystallization times in the isothermal crystallization; this indicated a faster crystallization of the polymer in the particle state and on the PVA substrate than that of the bulk sample. Furthermore, the polymers in the particle state and on the PVA substrate showed the preferential formation of the β-type crystalline form of PBA compared to the bulk one. The mechanism for the effects of the PVA layer or substrate on the crystallization kinetics and crystalline structure of PBA and its copolyesters are discussed. © 2013 Wiley Periodicals, Inc. J. Appl. Polym. Sci. **2014**, *131*, 39600.

KEYWORDS: biodegradable; crystallization; differential scanning calorimetry (DSC)

Received 11 April 2013; accepted 30 May 2013

DOI: 10.1002/app.39600

INTRODUCTION

Microparticles and nanoparticles of the biodegradable polymer have been widely used as drug-delivery vehicles.[1,2] These kinds of vehicles can sustain drug action to a disease and reduce the systematic side effects. They also have the advantages of easy extravasation into the tumor, good capability to cross various physiological barriers, and the controlled/targeted delivery of drugs. For the biodegradable microparticles and nanoparticles, the degradation rate is an important factor for their applications as drug carriers and vehicles. Several methods have been reported to control the degradation rate of polymer particles. For example, in the case of the D,L-lactide/glycolide copolymeric particles, the precise control of the degradation rate can be achieved by the adjustment of the molar ratio of D,L-lactide and glycolide monomers because the hydrolysis rate increases with increasing content of glycolide.[3]

A variety of methods have been developed to prepare the polymeric microparticles and nanoparticles.[1] Because the salting-out method prevents the use of surfactants and organic solvents and is thus friendly to the environment and the physiological system,[4] it has been a usual and feasible approach for preparing polymeric particles.[1] To stabilize the particles in the aqueous phase, the additive of stabilizer is frequently used in the salting-out process. Therefore, the surface of microparticles and nanoparticles prepared in the salting-out method is covered by the stabilizer; this enables the redispersion of particles in aqueous solution.

The crystalline structure of semicrystalline biodegradable polymers is one of important factors in the control over biodegradability.[5] An example is the polymorphic polyester of poly(butylene adipate) (PBA), which forms α, β, and α/β mixed crystals, under different crystallization temperatures (T_c's).[6–8] It has been found that the enzymatic biodegradation rate of PBA

Table I. Molecular Weights and Thermal Parameters of the PBA and PBHA Samples

Code	BA content (%)	HA content (%)[a]	M_w[b]	M_w/M_n[b]	T_m (°C)[c]	ΔH_m (J/g)[c]
PBA	100	0	1.2×10^4	1.33	51.3	76
PBHA16	84	16	1.6×10^4	1.33	46.0	79
PBHA26	74	26	1.5×10^4	1.50	37.4	83

[a] The comonomer composition of the PBHA copolymer was estimated via ^{1}H-NMR.
[b] M_w, weight-average molecular weight; M_n, number average molecular weight. The molecular weights of PBHA were measured via gel permeation chromatography with chloroform as the mobile phase.
[c] T_m and the enthalpy (ΔH_m) were obtained via DSC after the sample was melt-crystallized during a cooling process at 10°C/min.

relies on its crystalline structure, and it increases in the order α/β mixture $< \beta < \alpha$.[9] Therefore, controlling the crystalline structure of polymorphic polymer can be an effective approach in tailoring its biodegradation rate.

Because of the effects of the preparation condition and the additive (e.g., stabilizer), the biodegradable polymers can show different crystalline structures and crystallization behaviors in the microparticle/nanoparticle state from those in the bulk state. This will affect their degradation rates and functions in their application as drug vehicles. Therefore, to control the degradation rate and physical properties of polymeric microparticles and nanoparticles, it is of fundamental importance to clarify the crystalline structure and crystallization behavior of polymeric microparticles and nanoparticles. This, however, has not been explored to date.

PBA is a typical biodegradable polyester showing polymorphic crystalline structures. In a previous study, we synthesized a new kind of copolyester of PBA, that is, poly(butylene adipate-*co*-hexamethylene adipate) (PBHA).[10,11] The crystalline structure of PBHA depends not only on T_c but also on the comonomer content. This allows the feasible control of the biodegradation rate of PBHA. On the other hand, poly(vinyl alcohol) (PVA) is a common stabilizer for the preparation of microparticles and nanoparticles in the salting-out process because it is biocompatible, water-soluble, nonionic, nontoxic, and nonimmunogenic.[12] It has been used to prepare the monodispersed nanoparticles of poly(D,L-lactide) and poly(D,L-lactide-*co*-glycolide) in the salting-out method.[13]

In this study, we used PBA and PBHA as typical biodegradable polymorphic polymers and prepared biodegradable microparticles and nanoparticles by the salting-out technique using PVA as a macromolecular stabilizer. The crystallization kinetics and crystalline structure of PBA and PBHA in the particle state were investigated. To evaluate the effects of the PVA-covered layer, the crystallization kinetics and crystalline structure of PBA and PBHA on the surface of the PVA substrate were studied. The mechanism for the crystallization of PBA and PBHA in the particle state and on the PVA substrate is discussed. To our best knowledge, this is the first report to exploit the crystallization kinetics and crystalline structure of biodegradable polymeric particles.

EXPERIMENTAL

Materials

PBA was purchased from Sigma-Aldrich Co., Ltd. (St. Louis, MO) and was used without further purification. PBHA random polyesters were prepared according to a published method.[10] The comonomer composition, molecular weight, and thermal parameter of the PBHA copolymers are summarized in Table I. PVA film with a thickness of about 0.1 mm was prepared by the casting of an aqueous solution of PVA (2 wt %) in a glass dish, and then, water was evaporated under ambient conditions. The film was further dried at 100°C *in vacuo* for 24 h.

Preparation of the Polymer Microparticles and Nanoparticles

Microparticles and nanoparticles of PBA and its copolymers were fabricated by a salting-out method.[13] Typically, an acetone solution (5.0 g) containing 2 wt % polymer was poured into an aqueous solution (7.5 g) that contained 60 wt % $MgCl_2$ as the salting-out agent and 2 wt % PVA as the stabilizer. The mixture was then emulsified with an ultrasonic disruptor. After the fast addition of pure water (7.5 g) under ultrasonic mixing, the microparticles and nanoparticles were formed with the diffusion of the acetone to the water phase. The particles were separated by ultracentrifugation, purified by rinsing with water, and then lyophilized.

Scanning Electron Microscopy (SEM) Analysis

The morphology of the polyester particles was evaluated by a JSM-5200 scanning electron microscope (JEOL, Tokyo, Japan). The surface of the sample was coated by gold before the characterization.

Differential Scanning Calorimetry (DSC) Analysis

The crystallization and melting behavior of the polymer samples were investigated by a Pyris Diamond differential scanning calorimeter (PerkinElmer, Inc., Waltham, MA) under a nitrogen atmosphere. The samples were weighed and sealed in an aluminum pan. In the first scan, the sample was heated from −50 to 70°C. After melting at 70°C for 2 min, it was cooled to −50°C for the nonisothermal crystallization; this was followed by a reheating to 70°C. Both the cooling and heating rates were 10°C/min. In addition, after melting at 70°C for 2 min, the samples were quenched to the desired temperature under a cooling rate of 100°C/min and held at this temperature for isothermal crystallization. The period of isothermal crystallization was 30 min for PBA and 60 min for PBHA. The DSC curve in the isothermal crystallization process was recorded.

Fourier Transform Infrared (FTIR) Spectroscopy

FTIR spectra were measured on an IR spectrometer (Shimadzu, Kyoto, Japan) equipped with an AIM-8800 multichannel IR microscope (Shimadzu, Tokyo, Japan) and a mercury cadmium telluride (MCT) detector in the transmission mode. The sample

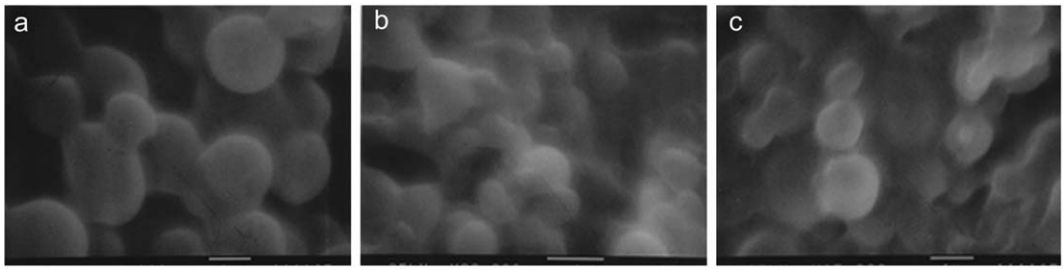

Figure 1. SEM micrographs of (a) PBA, (b) PBHA16, and (c) PBHA26 particles. The scale bars represent 1.0 μm.

was placed between two pieces of BaF_2 sheets and then melted at 100°C for 2 min; this was followed by quenching to the desired temperature for crystallization. FTIR spectra were collected after the completion of crystallization. All of the spectra were collected at 25°C to avoid temperature effects.

Wide-Angle X-Ray Diffraction (WAXD) Analysis

WAXD analysis was performed on a Rigaku RU-200 instrument (Rigaku Co., Tokyo, Japan) with a Ni-filtered Cu Kα radiation ($\lambda = 0.15418$ nm), working at 40 kV and 200 mA. The WAXD patterns were recorded in a 2θ range of 5–50° at a scanning rate of 2°/min. For the WAXD analysis, the film sample of the neat polymer was prepared by a hot press at 100°C and was then crystallized isothermally at the desired temperature. The as-prepared particle samples were coated on a glass slide and crystallized at different temperatures after melting at 70°C for 2 min. For the polymer crystallization on the PVA substrate, the polymer was first melted on a PVA film at 100°C and then cooled to the desired temperature for isothermal crystallization.

RESULTS AND DISCUSSION

Morphology of the Particles

Figure 1 shows the SEM images for the particles of PBA and its copolymers as prepared by the salting-out method. The particles were spherical, with a diameter of about 1.0 μm. It should be noted that the particles were interconnected to each other, possibly because of the adhesion of the PVA layer on the particle surface.

Crystallization of the Polymer in the Particle State

The crystallization kinetics and crystalline structure of the PBA and PBHA particles were investigated by DSC and WAXD. Figure 2(a,b) shows the DSC heating curves and WAXD patterns of the as-prepared polymer particles. All of the samples showed distinct melting peaks in the temperature range 30–60°C in the DSC curves and sharp diffraction peaks in the WAXD patterns; this indicated that the PBA and PBHA particles prepared in the salting-out process were semicrystalline. As shown in Figure 2(a), the melting temperature (T_m) of the polymer decreased with the incorporation of the hexamethylene adipate (HA) comonomer unit in PBA. This was attributable to the decrease of crystalline orderliness and the isomorphic crystallization of butylene adipate (BA) and HA units in the random copolyester of PBHA.[10,14] Despite the same preparation procedure, the PBA and PBHA particles showed a slightly different crystalline structure. As shown in Figure 2(b), except for the predominant diffraction of β-form crystals of PBA, the characteristic diffraction peaks of α-form PBA were also observed in the PBA particles, whereas only the diffraction peaks of the β-form PBA crystals were seen in the PBHA particles. This was consistent with our previous report, in which the β-form PBA-type crystals were preferable in the isomorphic crystallization of the PBHA copolymer, as compared to the PBA homopolymer.[10]

Figure 3 shows the DSC curves recorded in the nonisothermal melt crystallization and subsequent heating process for PBA and PBHA in the particle and bulk states. According to the

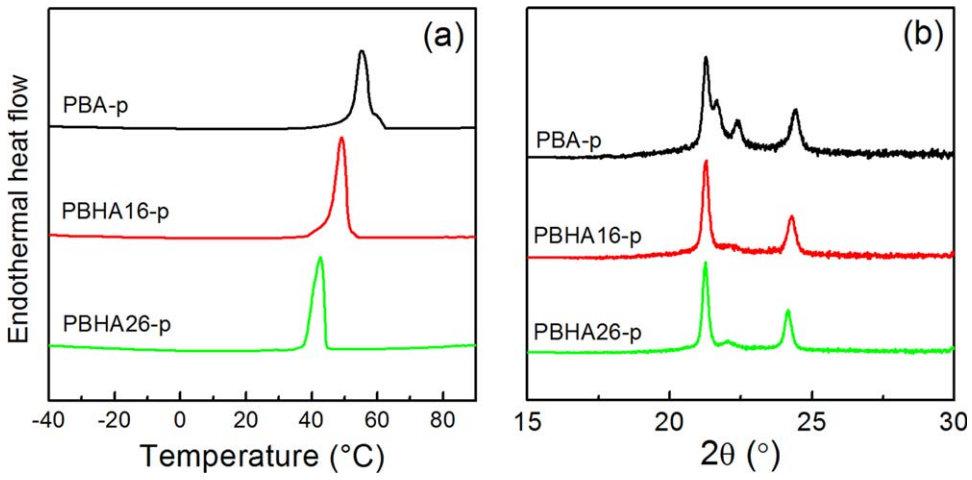

Figure 2. (a) DSC heating curves and (b) WAXD profiles of the particle samples of PBA and its copolymers. In the legend, "p" represents the particle sample. [Color figure can be viewed in the online issue, which is available at wileyonlinelibrary.com.]

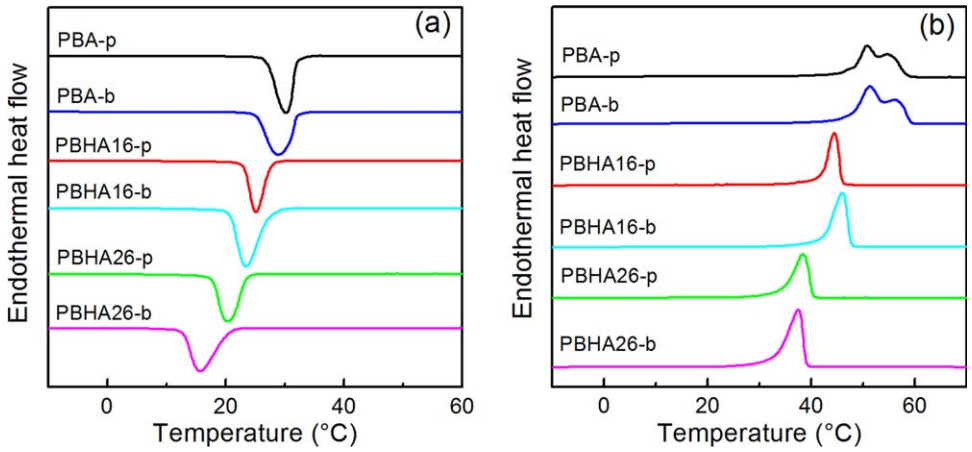

Figure 3. DSC curves recorded during (a) the cooling process and (b) the subsequent heating scans for the particle and bulk samples of PBA and its copolymers. In the legend, "p" and "b" represent the particle and bulk samples, respectively. [Color figure can be viewed in the online issue, which is available at wileyonlinelibrary.com.]

preparation procedure of the particles, the surfaces of the PBA or PBHA particles were coated and stabilized by a layer of PVA; this was also confirmed by the FTIR analysis (data not shown). Because PVA had a high glass-transition temperature of about 85°C and a high T_m of about 230°C, PBA and PBHA were encapsulated and confined by the PVA layer during the crystallization and thermal treatment. As shown in Figure 3, the polymer particles had different crystallization kinetics but similar melting behaviors with the bulk sample. It is interesting that the polymer particle had a higher T_c than the corresponding bulk sample; this was indicative of the faster crystallization of the former. This contradicted the general theory of confined crystallization, in which the crystallization rate of a polymer confined in a nanometer-scaled environment is usually decreased because of the difficulty of heterogeneous nucleation.[15–18]

The PBHA16 sample was used as an example to study the effects of particle formation on its crystalline structure. Figure 4(a) shows the WAXD profiles of the PBHA16 particles isothermally crystallized at different temperatures. Figure 4(b) shows the corresponding WAXD profiles of the bulk PBHA16. The WAXD profiles of the α- and β-form PBA are also included for comparison. Because BA was the major comonomer unit in PBHA16, the PBHA16 copolymer crystallized in the PBA-type crystals.[10] Similar to the PBA homopolymer, PBHA16 could form different crystalline polymorphs, depending on T_c. As shown in Figure 4(b), the β- and α-form PBA-type crystals were predominantly formed at T_c's of 25°C and T_c's greater than 34°C in bulk PBHA16, respectively. The mixture of the α- and β-form PBA-type crystals was formed at a T_c of 32°C. However, in the particle sample of PBHA16, the β- and α-form PBA-type crystals were mainly formed at T_c's of less than 32°C and greater than 36°C, respectively [Figure 4(a)]. As shown in Figure 4, the characteristic diffraction peak of the β(110) plane was observed in the PBHA16 particle sample crystallized at 34 and 36°C, whereas it was absent in the bulk sample crystallized under the same conditions. This implied that the β-form PBA-type crystals were preferably formed in the particle sample. On

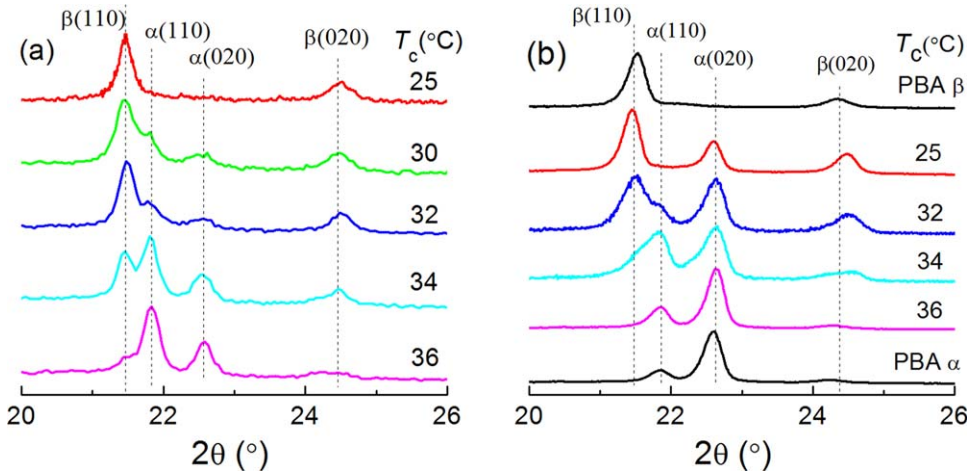

Figure 4. WAXD profiles of the (a) particle and (b) bulk samples of the PBHA16 melt-crystallized isothermally at different temperatures. [Color figure can be viewed in the online issue, which is available at wileyonlinelibrary.com.]

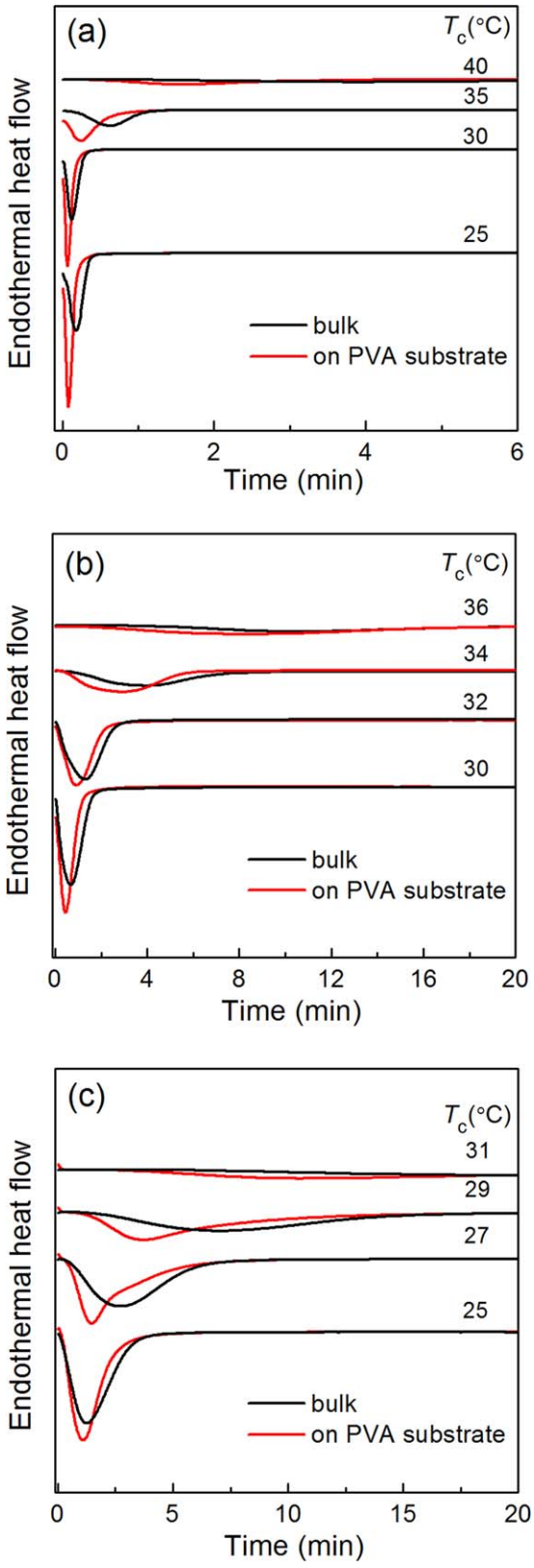

Figure 5. DSC curves recorded during the isothermal melt crystallization of (a) PBA, (b) PBHA16, and (c) PBHA26 (bulk and on PVA substrate). [Color figure can be viewed in the online issue, which is available at wileyonlinelibrary.com.]

the other hand, the particle and bulk samples crystallized at high T_c (e.g., 36°C) showed the different relative intensities of the α(110) and α(020) diffraction planes. The intensity of α(110) was much larger than that of α(020) in the particle sample crystallized at 36°C, which was opposite to that of the bulk sample crystallized under the same T_c. This may have been due to the different orientation of the spherulite and crystalline lamellae formed in the particle and bulk states.

Crystallization of the Polymer on the PVA Substrate

To explain the unique crystallization kinetics and crystalline structure of polymer particles covered by the PVA layer, we further studied the crystallization of PBA and its copolymer on the PVA substrate. Figure 5 shows the DSC curves of PBA and PBHA in the bulk state and on the PVA substrate during the isothermal melt crystallization at different temperatures. The crystallization peak of the polymer crystallized on the PVA substrate was sharper and shifted to the smaller time side, as compared to that of the bulk sample. This indicated the faster crystallization of PBA and PBHA on the PVA substrate, similar to the crystallization kinetics results of the PBA and PBHA particles.

To evaluate the isothermal crystallization kinetics, the heat flow in the isothermal DSC curve was integrated to attain the relative degree of crystallinity (X_t) at different crystallization times (t's). X_t was calculated from the integrated area of the DSC curve from $t = 0$ to $t = t$, divided by the integrated area of whole heat flow curve. A horizontal line from a point after the crystallization exotherm was used as the baseline for integration. The half-time of crystallization ($t_{0.5}$) was evaluated from the time with $X_t = 50\%$. The value of $1/t_{0.5}$ was used to denote the crystallization rate. Figure 6 shows the plot of $1/t_{0.5}$ versus T_c for the PBA and PBHA crystallized in the bulk state and on the PVA substrate. Under the same T_c, PBA and PBHA crystallized on the PVA substrate exhibited a larger crystallization rate than those crystallized in the bulk state. Because of the difficulty of nucleation at high T_c, the crystallization rate decreased as T_c increased.

On the basis of the results of isothermal crystallization, the crystallization kinetics of PBA and its copolymer crystallized under different conditions were further evaluated by the Avrami model. The linear form of the Avrami equation can be stated as follows:[19]

$$\log[-\ln(1-X_t)] = \log k + n \log t$$

where n is the Avrami index and k is the overall rate constant associated with both nucleation and growth contributions. We found that PBA and PBHA crystallized in the bulk state and on the PVA substrate had the similar n values; these were in the range 2.4–2.8. However, PBA and PBHA crystallized on the PVA substrate had larger k values than those crystallized in the bulk state, in agreement with the results of $t_{0.5}$.

The effects of the PVA substrate on the crystalline structure of PBA and PBHA were studied by WAXD and FTIR analysis. Figure 7 shows the WAXD patterns and FTIR spectra within the wave-number range 1000–850 cm^{-1} for PBHA16 crystallized on the PVA substrate at different temperatures. By comparing the

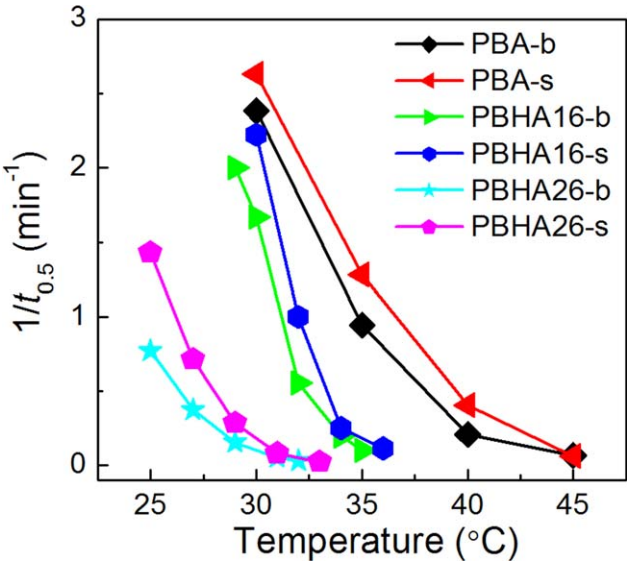

Figure 6. $t_{0.5}$ of PBA and its copolymer at different T_c's. In the legend, "b" and "s" represent the bulk sample and the sample crystallized on a PVA substrate, respectively. [Color figure can be viewed in the online issue, which is available at wileyonlinelibrary.com.]

WAXD profiles shown in Figures 7(a) and 4(b), we observed the different T_c dependences of the crystalline structure for the polymer crystallized in the bulk state and on the PVA substrate. For the PBHA16 crystallized on the PVA substrate, the neat β-form, α-form, and α/β mixed PBA-type crystals were formed at $T_c = 25$–32°C, $T_c > 36$°C, and $T_c = 34$°C, respectively. As shown in Figure 7(b), the relative intensity of 930 cm^{-1}, associated with the stretching vibrations of the C—C backbone in the β-form crystals,[20,21] was almost invariant with the T_c in the range 25–32°C, whereas it decreased as T_c increased to 34°C and disappeared at $T_c = 36$°C. This was consistent with the WAXD results. When we compared the T_c-dependent crystalline structure of the bulk sample, we concluded that the PVA substrate promoted the crystallization of the β-form PBA-type crystals in PBHA.

To compare the T_c-dependent crystalline structure of PBA and PBHA under the different crystallization conditions, the relative area of the PBA β[(110)+(020)] and α[(110)+(020)] diffraction planes for the bulk and particle samples, and the samples crystallized on the PVA substrate were roughly evaluated by the calculation of the relative integrated intensities of the diffraction peaks of the PBA β[(110)+(020)] and α[(110)+(020)] planes in the WAXD patterns. The value of $\beta[(110)+(020)]/\{\beta[(110)+(020)]+\alpha[(110)+(020)]\}$ represents the relative fraction of the β-form crystals in the crystalline phase; this is plotted as a function of T_c in Figure 8. As shown in this figure, the relative fraction of β-form crystals decreased with increasing T_c. Under the same T_c, the relative fraction of the β-form crystals was highest when the sample was crystallized in the particle state that was covered by the PVA layer.

Plausible Mechanism for PVA Effects on the Polymorphic Crystallization of PBA and PBHA

Because the polymer particles as-prepared were coated by a PVA layer, it was reasonable to consider that the unique crystallization kinetics and polymorphism of PBA and its copolymers in the particle state and on PVA substrate were induced by PVA. All of the results indicate that the PVA layer and substrate not only enhanced the crystallization rate but also promoted the formation of the β-form PBA-type crystals in the PBA and its copolymer. A possible reason was that the interface between PVA and PBA or its copolymer enhanced the nucleation in crystallization; this was caused by a decrease in the surface free energy of formation of crystal nuclei because of the presence of the phase interface.[22–25] The decrease in the surface energy accelerated the nucleation and improved the mobility of the polymer chain near the interface.[26] On the other hand, Yan and coworkers[27,28] reported that the oriented polyethylene and isotactic polypropylene substrates induced the exclusive formation of β-form crystals of PBA because of epitaxial crystallization. We propose that the preferential crystallization of the β-form PBA-type crystals may have also been due to their epitaxial crystallization and growth on the PVA surface; this was due to the presumable interactions between PVA and PBA or its copolymers, for example, the H-bond interactions between the hydroxyl groups of

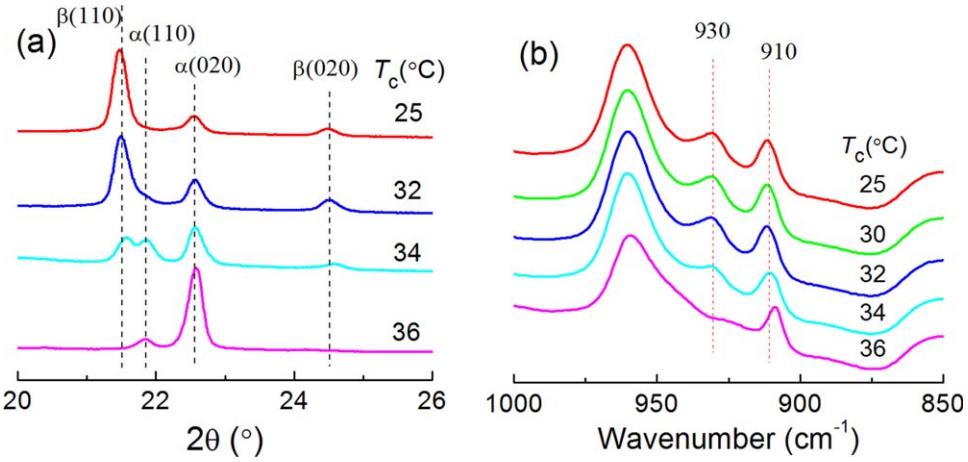

Figure 7. (a) WAXD profiles and (b) FTIR spectra of the PBHA16 melt-crystallized isothermally on a PVA substrate at different temperatures. [Color figure can be viewed in the online issue, which is available at wileyonlinelibrary.com.]

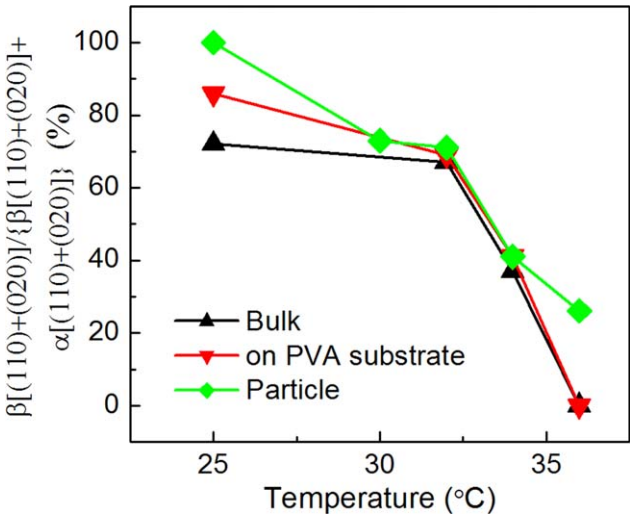

Figure 8. Plot of $\beta[(110) + (020)]/\{\beta[(110) + (020)] + [(110) + \alpha(020)]\}$ versus T_c for PBHA16 crystallized under different crystallization conditions. [Color figure can be viewed in the online issue, which is available at wileyonlinelibrary.com.]

PVA and the carbonyl groups of polyester. More in-depth experiments will be performed in the future to verify this proposal.

CONCLUSIONS

The crystallization kinetics and crystalline structure of the biodegradable polymorphic polymers of PBA and PBHA in the particle state and on the PVA substrate were investigated. The PBA and PBHA in the particle state and on the PVA substrate showed faster crystallization than the bulk polymers. The polymers in the particle state and on the PVA substrate showed the preferential formation of the β-form PBA-type crystals in comparison to the bulk sample. We proposed that the effects of the PVA layer or substrate on the crystallization kinetics and crystalline structure of PBA and PBHA were due to the lowering surface free energy for nucleation and the possible epitaxial growth of the β-form PBA-type crystals on the PVA surface. This study has provided a new method for manipulating the crystallization kinetics and crystalline structure of the polymorphic biodegradable polymers and allowing for the control over biodegradation rate of polymeric particles.

ACKNOWLEDGMENTS

One of the authors (P.P.) is grateful for the financial support from the National Natural Science Foundation of China (contract grant numbers 51103127 and 21274128) and the State Key Laboratory of Chemical Engineering (contract grant numbers SKLChE-11D05 and SKL-ChE-12D06).

REFERENCES

1. Rao, J. P.; Geckeler, K. E. *Prog. Polym. Sci.* **2011**, *36*, 887.
2. Soppimath, K. S.; Aminabhavi, T. M.; Kulkarni, A. R.; Rudzinski, W. E. *J. Controlled Release* **2001**, *70*, 1.
3. Gilding, D. K.; Reed, A. M. *Polymer* **1979**, *20*, 1459.
4. Bindschaedler, C.; Gurny, R.; Doelker, E. U.S. *Pat. 4*,968,350 (**1990**).
5. Pan, P.; Inoue, Y. *Prog. Polym. Sci.* **2009**, *34*, 605.
6. Gan, Z.; Abe, H.; Doi, Y. *Macromol. Chem. Phys.* **2002**, *203*, 2369.
7. Gan, Z.; Kuwabara, K.; Abe, H.; Iwata, T.; Doi, Y. *Biomacromolecules* **2004**, *5*, 371.
8. Woo, E. M.; Wu, M. C. *J. Polym. Sci. Part B: Polym. Phys.* **2005**, *43*, 1662.
9. Gan, Z.; Kuwabara, K.; Abe, H.; Iwata, T.; Doi, Y. *Polym. Degrad. Stab.* **2005**, *87*, 191.
10. Liang, Z.; Pan, P.; Zhu, B.; Inoue, Y. *Macromolecules* **2010**, *43*, 6429.
11. Liang, Z.; Pan, P.; Zhu, B.; Yang, J.; Inoue, Y. *Polymer* **2011**, *52*, 5204.
12. Chiellini, E.; Corti, A.; D'Antone, S.; Solaro, R. *Prog. Polym. Sci.* **2003**, *28*, 963.
13. Zweers, M. L. T.; Grijpma, D. W.; Engbers, G. H. M.; Feijen, J. *J. Biomed. Mater. Res. Part B* **2003**, *66*, 559.
14. Liang, Z.; Pan, P.; Zhu, B.; Dong, T.; Hua, L.; Inoue, Y. *Macromolecules* **2010**, *43*, 2925.
15. Tol, R. T.; Mathot, V. B. F.; Groeninckx, G. *Polymer* **2005**, *46*, 383.
16. Muller, A. J.; Balsamo, V.; Arnal, M. L.; Jakob, T.; Schmalz, H.; Abetz, V. *Macromolecules* **2002**, *35*, 3048.
17. Pan, P.; Zhao, L.; Zhu, B.; He, Y.; Inoue, Y. *J. Appl. Polym. Sci.* **2010**, *117*, 3013.
18. Pan, P.; Zhao, L.; Yang, J.; Inoue, Y. *Macromol. Mater. Eng.* **2013**, *298*, 201.
19. Gedde, U. W. Polymer Physics; Chapman & Hall: London, **1995**; p 169.
20. Yang, J.; Li, Z.; Pan, P.; Zhu, B.; Dong, T.; Inoue, Y. *J. Polym. Sci. Part B: Polym. Phys.* **2009**, *47*, 1997.
21. Yang, J.; Pan, P.; Hua, L.; Zhu, B.; Dong, T.; Inoue, Y. *Macromolecules* **2010**, *43*, 8610.
22. Bartczak, Z.; Galeski, A.; Krasnikova, N. P. *Polymer* **1987**, *28*, 1627.
23. Wenig, W.; Asresahegn, M. *Polym. Eng. Sci.* **1993**, *33*, 877.
24. Tsuburaya, M.; Saito, H. *Polymer* **2004**, *45*, 1027.
25. Zhang, X.-H.; Wang, Z.-G.; Muthukumar, M.; Han, C. C. *Macromol. Rapid Commun.* **2005**, *26*, 1285.
26. Sakai, F.; Nishikawa, K.; Inoue, Y.; Yazawa, K. *Macromolecules* **2009**, *42*, 8335.
27. Sun, Y.; Li, H.; Huang, Y.; Chen, E.; Zhao, L.; Gan, Z.; Yan, S. *Macromolecules* **2005**, *38*, 2739.
28. Sun, Y.; Li, H.; Huang, Y.; Chen, E.; Gan, Z.; Yan, S. *Polymer* **2006**, *47*, 2455.